unique changeover from n-type to p-type conduction as the temperature is raised. If the p-type carrier has a greater mobility than the n-type, then it can become dominant at higher temperature if its excitation energy is higher than that of the n-type carrier. A consistent model for blue KMo bronze would be that the low-temperature conductivity is dominated by electron hopping or electron excitation from donor centers into a narrow, low-mobility conduction band, while the high-temperature conductivity is dominated by hole conduction in a high-mobility valence band. The narrow conduction band could develop from small overlap of 4d t_{2g} orbitals between Mo atoms; the wide valence band, from large overlap of 4d t_{2g} Mo orbitals and oxygen $p\pi$ orbitals. Oxygen atoms that are bridge atoms between clusters could be centers for hole-type excitation, since removal of one electron from this site could make other binding electrons in the O–Mo–O–Mo–O molecular orbitals highly mobile. The two-carrier model suggests interesting photoconductive properties, and, indeed, a large photoconduction response has been observed.

The behavior of the Seebeck coefficient is qualitatively in agreement with the conductivity results. Below 180°K, Q is negative and rapidly becomes more negative as the temperature is decreased. Such a rapid decrease in Q is typical of an n-type semiconductor in which carrier density exponentially decreases with decreasing temperature. (For semiconductors, Q is roughly proportional to the reciprocal of the log of the carrier density.) Above 180°K, Q is very small and shows practically no change with temperature; this is consistent with metallic behavior. No special significance should be attached to the fact that Q is still negative in the range where the Hall voltage has already turned positive. It is not unusual (*cf.* NiO, Cu_2O) to have opposite signs for Q and the Hall voltage, particularly when phonon drag is important. The rather steep change to a substantial positive Q at 298°K, although consistent with p-type carriers, is not understood at the present time. It will be investigated further.

There is the final possibility that the observed changes are associated with structural changes in the critical regions $140°K < T < 180°K$ and 292–298°K. Dta analysis, however, with equipment sensitive to 0.0001 cal, showed no first-order changes and only the barest trace of a second-order change at about 160°K.

CONTRIBUTION FROM THE DEPARTMENT OF CHEMICAL ENGINEERING,
THE UNIVERSITY OF TEXAS, AUSTIN, TEXAS

The Crystal Chemistry of Selected AB_2 Rare Earth Compounds with Selenium, Tellurium, and Antimony[1]

BY R. WANG AND H. STEINFINK

Received January 16, 1967

The rare earth ditellurides, diselenides, and diantimonides were synthesized and their crystal structures were investigated. The ditellurides are isostructural and have the Fe_2As (C38) structure. The phases $HoTe_2$ and $ErTe_2$ do not exist and reasons for their absence are given. The structures of the diselenides display two types of supercells. The lighter rare earths have a tetragonal cell and the heavier ones have an orthorhombic cell, but the subcell has an arrangement which is identical with the telluride structure. The diantimonides are formed by a limited number of rare earths and they crystallize with a new structure which, however, is closely related to the $RETe_2$ type and to the $ZrSi_2$ structure. The phase $YbSb_2$ crystallizes in the latter type. The interrelationships among these structures and the nature of the bonding existing in these compounds is discussed.

Introduction

The stoichiometry REB_2, where RE is a rare earth element and B an element of groups V and VI, is widely encountered in such alloys. A structural investigation of these phases was undertaken, using single-crystal X-ray diffraction techniques wherever feasible, to determine their crystal structures and resolve any ambiguities which have arisen because of previous work which was based only on powder diffraction diagrams.

Rare earth diselenides were first prepared by Benacerraf, *et al.*,[2] and from chemical analyses they assigned the formula RE_2Se_4 to the La, Ce, Pr, and Nd compositions and the formula $RE_2Se_{3.6}$ to compounds of Sm and Gd. Powder patterns indicated that the unit cell was tetragonal and the lattice constants were determined. Vickery and Muir[3] studied $GdSe_2$ and reported that a low-temperature modification of this phase had the $ThSe_2$ type of structure. Veale and Barrett[4] found that in the Gd–Se system the phase exists only over the stoichiometry range $GdSe_{1.775-1.862}$ and the powder pattern cannot be indexed on an orthorhombic unit cell similar to $ThSe_2$ but has a tetragonal unit cell. Many diselenides and ditellurides display a solid solution

(1) Research sponsored by Air Force Office of Scientific Research, Office of Aerospace Research, U. S. Air Force, Grant No. 806-65.

(2) A. Benaceraff, L. Domange, and J. Flahaut, *Compt. Rend.*, **248**, 1672 (1959).

(3) R. C. Vickery and H. M. Muir, "Rare Earth Research," E. V. Kleber, Ed., The Macmillan Co., New York, N. Y., 1961, p 223.

(4) C. R. Veale and M. F. Barrett, *J. Inorg. Nucl. Chem.*, **28**, 2161 (1966).

range owing to a deficiency of the B atom and Wang, *et al.*,[5] have shown that the missing atoms in the ditellurides come from the close-packed tellurium layer in the structure. Recently Eliseev and Kuznetzov[6] and Yarembash, *et al.*,[7] have investigated single crystals of MSe_{2-x} (M = La, Pr, Nd) and report that they are isostructural with $LaTe_2$. Haase, *et al.*,[8] found that single-crystal X-ray diagrams of $ErSe_2$ display weak diffraction spectra which make the true symmetry orthorhombic although the strong intensities can be indexed on the basis of a tetragonal cell similar to that of $LaTe_2$ and that the structure of $ErSe_2$ within the subcell is the same as for $LaTe_2$. The supercell is considered due to ordering of vacancies in the nonstoichiometric compounds.

The rare earth ditellurides have been studied by several investigators and they are all isostructural and have the Fe_2As (C38) structure.[5,9-11] Miller, *et al.*,[12] prepared $GdTe_2$ by a vapor deposition method and reported a tetragonal unit cell, $a = 9.10$ A, $c = 9.30$ A, which differs from the values of the a axes (~4.5 A) usually reported for the ditellurides. No further structure investigation was carried out for this compound.

The rare earth diantimonides have received very little attention and only the two systems La–Sb[13] and Yb–Sb[14] have been studied. In both, the diantimonides were present, and Wang, *et al.*,[15] have reported that $YbSb_2$ is isostructural with $ZrSi_2$.

Experimental Section

The ditellurides $LaTe_2$, $CeTe_2$, $NdTe_2$, $SmTe_2$, $GdTe_2$, $DyTe_2$, and $YbTe_2$ were prepared by methods previously described,[8] and both single-crystal and powder diffraction data showed that they are all isostructural and have the Fe_2As type of structure. The phases $ErTe_2$ and $HoTe_2$ were absent and attempts to synthesize them produced mixtures of RETe and $RETe_3$.

The compounds $LaSe_2$, $CeSe_2$, $NdSe_2$, $SmSe_2$, $GdSe_2$, $DySe_2$, $HoSe_2$, and $ErSe_2$ were prepared from the elements by sealing the stoichiometric amounts in evacuated Vycor tubes and heating at reaction temperatures below 800°. The compounds thus obtained are labeled with the formula $RESe_2$ even though they may exhibit nonstoichiometric compositions; *i.e.*, they may be selenium deficient. $GdSe_2$ was also prepared at a temperature under 300°. The reaction was very slow and 2 weeks was required to carry it to completion. The low-temperature product gave a homogenous X-ray powder pattern which displayed no difference when compared with the pattern from the high-temperature preparation and we consider that $GdSe_2$ does not have a high–low temperature phase transition up to at least 800°. All attempts to prepare $YbSe_2$ by preheating the metal with the proper amount of selenium in a Vycor tube below 400° for 2 days and at final reaction temperatures between 400 and 800° were unsuccessful, and the diffraction patterns of the products showed the existence of two phases, cubic YbSe and Se.

Crystals of $LaSb_2$, $CeSb_2$, $NdSb_2$, $SmSb_2$, and $YbSb_2$ were prepared by allowing the rare earth elements and antimony to react in evacuated Vycor tubes. The samples were preheated below 500° for 48 hr and kept later at 700–750° for about 1 week. Good crystalline phases were obtained. The compounds $LaSb_2$, $NdSb_2$, and $YbSb_2$ were also successfully prepared by a liquid–liquid reaction in tantalum tubes at about 1500°. These compounds are very stable under atmospheric conditions. Crystals of $LaSb_2$ were heated to 1000° for 24 hr and quenched in water. No phase transition occurred.

Results

Well-formed single crystals suitable for X-ray diffraction studies could be found for $SmSe_2$, $GdSe_2$, $DySe_2$, $HoSe_2$, and $ErSe_2$ and their patterns were essentially identical. Approximately 80% of the *hkl* reflections whose intensities ranged from weak to strong had indices $h = 2n$, $k = 4n$, and $l = 3n$; the other 20% were very weak and had indices $h + k = 2n$, and all values of l were present. For *hk*0 reflections only those with indices $h = 2n$ and $k = 4n$ were observed, 0*kl* reflections $k = 4n$ and $l = 3n$ existed, and *h*0*l*, $h = 2n$, and $l = 3n$ could be seen. The true diffraction symmetry, considering all reflections, was mmmC--*a*, although the large number of absent reflections places doubt on the *a* glide, and it was evident that an orthorhombic superstructure cell existed as well as a tetragonal subcell which were related by $a_{super} = 2c_{sub}$, $b_{super} = 4a_{sub}$, and $c_{super} = 3a_{sub}$. The subcell was tetragonal and the space group P4/nmm could be derived from the observed extinctions.

The preparative conditions used here produced only very small crystals for the compounds $LaSe_2$, $CeSe_2$, and $NdSe_2$ which were not suitable for single-crystal techniques. Their powder patterns resembled each other as well as the powder patterns of the other phases except that several very faint lines which occur in the $ErSe_2$ type of pattern and which are indexed on the basis of an orthorhombic cell were not observed. The complete powder patterns of $LaSe_2$, $CeSe_2$, and $NdSe_2$ can be indexed by a smaller superstructure cell having two basic $RETe_2$ unit cells attacked along both the *a* and *b* axes and the space group P4/nmm is still valid. Table I lists the crystallographic data for the diselenides as determined in this investigation.

Refinement of the Structure of $ErSe_2$

A single-crystal of $ErSe_2$ ($\mu_{MoK\alpha} = 593$ cm^{-1}) with approximate dimensions 0.08 × 0.04 × 0.01 mm was selected for examination. The crystal was mounted along the *a* axis of the tetragonal subcell and three-dimensional intensities were collected with filtered molybdenum radiation using multiple-film Weissenberg exposures. Among the observed reflections were 45 very weak ones due to the superlattice. The intensities were obtained by visual comparison with a graduated intensity scale prepared from timed exposures of a reflection from the single crystal; the Lorentz and polarization corrections were applied but no absorption corrections were made. The scattering factors for Er and Se as given in the "International Tables for X-

(5) R. Wang, H. Steinfink, and W. F. Bradley, *Inorg. Chem.*, **5**, 142 (1966).
(6) A. A. Eliseev and V. G. Kuznetzov, *Neorgan. Materiali*, **2**, 1157 (1966).
(7) E. I. Yarembash, A. A. Eliseev, V. I. Kalitin, and L. I. Antonova, *ibid.*, **2**, 984 (1966).
(8) D. J. Haase, H. Steinfink, and E. J. Weiss, *Inorg. Chem.*, **4**, 538 (1965).
(9) L. Domange, J. Flahaut, M. P. Pardo, A. N. Chirezi, and M. Guittard, *Compt. Rend.*, **250**, 875 (1960).
(10) M. P. Pardo, J. Flahaut, and L. Domange, *Bull. Soc. Chim. France*, 3267 (1964).
(11) W. Lin, H. Steinfink, and E. J. Weiss, *Inorg. Chem.*, **4**, 877 (1965).
(12) J. F. Miller, F. J. Reid, L. K. Matson, J. W. Moody, R. D. Baxter, and R. C. Himes, Technical Documentary Report No. ALTDR 64-239, Battelle Memorial Institute, 1964, p 16.
(13) R. Vogel and H. Klose, *Z. Krist.*, **A97**, 223 (1936).
(14) R. E. Bodnar and H. Steinfink, *Inorg. Chem.*, **6**, 327 (1967).
(15) R. Wang, R. E. Bodnar, and H. Steinfink, *ibid.*, **5**, 1468 (1966).

TABLE I

CRYSTALLOGRAPHIC DATA OF RARE EARTH DISELENIDES (λ 1.542 A)

Compound	Structure type	Lattice constants, A			No. of formula wt/ unit cell	Dimension of subcell, A		Vol, A³	Mean atomic vol, A³/atom
		a	b	c		a_{sub}	c_{sub}		
$LaSe_2$	$LaSe_2$	8.468		8.529	8	4.234	8.529	611.6	25.48
$CeSe_2$	$LaSe_2$	8.439		8.489	8	4.219	8.489	604.5	25.19
$NdSe_2$	$LaSe_2$	8.273		8.330	8	4.137	8.330	570.1	23.75
$SmSe_2$	$ErSe_2$	16.49	16.18	12.14	48	4.046	8.244	3239.1	22.49
$GdSe_2$	$ErSe_2$	16.47	16.08	12.06	48	4.020	8.233	3193.9	22.18
$DySe_2$	$ErSe_2$	16.39	15.94	11.96	48	3.985	8.193	3124.6	21.70
$HoSe_2$	$ErSe_2$	16.37	15.92	11.94	48	3.980	8.188	3111.7	21.61
$ErSe_2$	$ErSe_2$	16.36	15.90	11.92	48	3.975	8.184	3100.7	21.53

Ray Crystallography,"[16] corrected for the real part of the dispersion only, were used in the calculation.

The small number of reflections from the true structure, 45, was insufficient to permit the solution of the superstructure. Many models in space group Cmma, as well as structures fitting into other space groups, were tried but none gave satisfactory agreement between all observed and calculated structure factors.

The assumption of the same space group and atomic positions as found in $RETe_2$[5] permitted the subcell structure to be refined to $R = \Sigma||F_o| - |F_c||/\Sigma|F_o| = 0.13$ for 121 independent reflections greater than zero. The refinement was carried out using the least-squares program by Busing, Martin, and Levy,[17] using unit weight for all structure factors with observable values and zero for others. The standard deviation of an observation, $[\Sigma w(F_o - F_c)^2/(n_o - n_v)]^{1/2}$, is 1.23 where $n_o = 121$, the number of reflections, and $n_v = 35$, the total number of variables adjusted to the data set. The reflections from each level were refined separately by using a set of atomic parameters obtained from a zero-level refinement. The sets of scaled F_o obtained in this manner were combined and an over-all refinement was carried out. The new set of atomic parameters was then used to recalculate scaled F_o values for each level separately and they were then recombined for the next over-all refinement. This procedure was repeated until no further changes in atomic parameters and scaled F_o occurred. Only isotropic temperature factors were used in these steps until the scaling was complete. The F_o and F_o and coordinates from the final refinement of the subcell structure using anisotropic temperature factors are given in Tables II and III, respectively. The Se(2) atom exhibits strong thermal vibration anisotropy. (This is similar to the Te in the basal plane of the $NdTe_2$ structure[5] and a refinement on the occupancy factor resulted in a value of 0.9. The absence of an absorption correction makes it difficult to assess the significance of the deviation from unity, but the parallel behavior of this atom with the corresponding Te in $NdTe_2$ lends support that the thermal anisotropy is real.)

(16) "International Tables for X-Ray Crystallography," Vol. 3, The Kynoch Press, Birmingham, England, 1962.

(17) W. R. Busing, K. O. Martin, and H. A. Levy, USAEC Report ORNL TM-305, Oak Ridge National Laboratory, Oak Ridge, Tenn., 1962.

TABLE II

OBSERVED AND CALCULATED STRUCTURE FACTORS FOR THE $ErSe_2$ TETRAGONAL SUBCELL[a]

h = 0, k = 0

l	F_o	F_c
1	0	0
2	50	-63
3	123	135
4	67	78
5	0	3
6	0	-1
7	55	52
8	77	61
9	0	-21
10	0	7
11	58	48

h = 0, k = 1

l	F_o	F_c
1	77	74
2	19	-21
3	95	118
4	32	-40
5	78	-87
6	72	77
7	17	18
8	64	-49
9	0	-5
10	0	-17
11	0	1

h = 0, k = 2

l	F_o	F_c
0	151	178
1	19	-16
2	64	67
3	101	94
4	49	53
5	0	-9
6	0	-11
7	40	38
8	52	47
9	0	-26
10	0	
11	58	49

h = 0, k = 3

l	F_o	F_c
1	61	53
2	17	13
3	84	86
4	29	-30
5	68	-67
6	68	62
7	21	-14
8	37	-40

h = 0, k = 4

l	F_o	F_c
0	105	103
1	29	-25
2	55	-60
3	52	52
4	33	26
5	0	-17
6	0	-19
7	0	20
8	27	29

h = 0, k = 5

l	F_o	F_c
1	32	35
2	0	8
3	61	-58
4	0	21
5	41	47
6	43	-44
7	0	-20
8	0	30

h = 0, k = 6

l	F_o	F_c
0	65	65
1	0	-19
2	33	-42
3	35	32

h = 1, k = 1

l	F_o	F_c
0	140	-125
1	95	92
2	133	143
3	48	-40
4	0	0
5	48	59
6	45	56
7	0	-2
8	17	-17
9	64	55
10	10	22

h = 1, k = 2

l	F_o	F_c
1	75	61
2	19	15
3	107	-98
4	43	34
5	96	75
6	73	-69
7	0	-16
8	35	44
9	0	-5

h = 1, k = 3

l	F_o	F_c
0	123	-105
1	62	47
2	117	87
3	42	-45
4	0	-15
5	36	33
6	34	33
7	0	-12
8	20	-23
9	38	39

h = 1, k = 4

l	F_o	F_c
1	46	-42
2	0	-10
3	74	69
4	30	-25
5	65	-55
6	56	52
7	0	12
8	32	-35

h = 1, k = 5

l	F_o	F_c
0	73	-77
1	35	25
2	57	53
3	38	-37
4	0	-16
5	0	18
6	0	19
7	0	-13
8	0	-21

h = 1, k = 6

l	F_o	F_c
1	0	-28
2	0	-7
3	43	47

h = 2, k = 2

l	F_o	F_c
0	151	141
1	18	-23
2	70	-66
3	83	73
4	48	39
5	51	-14
6	18	-16
7	29	29
8	37	39

h = 2, k = 3

l	F_o	F_c
1	55	-47
2	18	-11
3	90	77
4	31	-27
5	70	-61
6	61	56
7	0	13
8	33	37

h = 2, k = 4

l	F_o	F_c
0	100	92
1	28	-24
2	54	-56
3	49	46
4	33	22
5	0	-17
6	0	-18
7	0	17
8	0	26

h = 2, k = 5

l	F_o	F_c
1	31	32
2	0	8
3	52	-54
4	0	19
5	48	44
6	43	-41
7	0	-10
8	41	28

h = 2, k = 6

l	F_o	F_c
0	44	61
1	0	-18
2	31	-40
3	26	30

h = 3, k = 3

l	F_o	F_c
0	97	-90
1	38	32
2	73	65
3	42	-42
4	0	-17
5	21	23
6	31	24
7	0	-13
8	29	-23

h = 3, k = 4

l	F_o	F_c
1	43	-35
2	0	-8
3	60	58
4	0	-21
5	46	-47
6	44	44

h = 3, k = 5

l	F_o	F_c
0	69	-67
1	23	21
2	51	45
3	48	-32

h = 3, k = 6

l	F_o	F_c
1	27	-24
2	0	-6
3	41	41

[a] Unobserved values of F_o are shown as zero and were not used in the refinement and in the calculation of R. The noncentrosymmetric origin is used and the signs shown for F_o represent the phase of $A(hkl)$ when $h + k = 2n$ and of $B(hkl)$ when $h + k = 2n + 1$.

TABLE III
FINAL PARAMETERS AND THEIR STANDARD DEVIATIONS FOR $ErSe_2$ SUBSTRUCTURE

	x	y	z	$B_{11} = B_{22}$	B_{33}
Er	0	0.5	0.7265 ± 0.0007	0.0074 ± 0.0016	0.0077 ± 0.0008
Se(1)	0	0.5	0.3666 ± 0.0016	0.0069 ± 0.0039	0.0069 ± 0.0019
Se(2)	0	0	0	0.0263 ± 0.0312	0.0031 ± 0.0025

Discussion of the Structure

In an extensive review of oxides and chalcogenides, Anderson[18] found that in most cases they form nonstoichiometric compounds; frequently they exhibit a range of composition, and among them many superstructures exist. By analogy with the $RETe_2$ structure which has a tendency to lose Te atoms from the basal plane, it is reasonable to believe that selenium atoms are also missing in $RESe_2$ compounds. If the defects in $RESe_2$ are ordered instead of disordered as in some $RETe_2$ solid solutions, weak X-ray diffraction spots indicative of this type of ordering will be observed and lead to the identification of a superstructure. The structures of $RESe_2$ can be considered as superstructures based on the $RETe_2$ structure with a large number of point defects (or vacancies) which are ordered in the structure. This conclusion is consistent with the observations of Benacerraf, *et al.*,[2] who state that only $Sm_2Se_{3.6}$ and $Gd_2Se_{3.6}$ nonstoichiometric compounds can be found, and of Veale and Barrett,[4] who found that the phase "$GdSe_2$" had a composition which ranged from $GdSe_{1.775}$ to $GdSe_{1.862}$.

The z parameters of the atoms in the $ErSe_2$ subcell have almost the same values as those for $LaTe_2$ and $NdTe_2$.[5] The thermal motions in both structures are quite similar; the Se(2) atoms in the basal plane have also larger temperature factors along the x and y directions than the z direction. Since the selenium atoms are smaller than the tellurium atoms, the interatomic distances in $ErSe_2$ are of interest and they are listed in Table IV.

TABLE IV
INTERATOMIC DISTANCES IN $ErSe_2$, A

Se(2)–Se(2)	2.811
Se(1)–Se(2)	3.603 ± 0.009
Se(1)–Se(1)	3.553 ± 0.013
Er–Se(2)	2.990 ± 0.004
Er–Se(1)	2.945 ± 0.010
Er–Se(1)	2.915 ± 0.010

The Se(2)–Se(2) distance in the basal plane is quite short; the atomic radius of Se calculated from this separation is 1.405 A which indicates that the bonding is partially ionic and partially covalent in character (the covalent radius for Se is 1.17 A).

The $RESb_2$ Structures

The structure of $YbSb_2$ is isostructural with $ZrSi_2$ and a detailed discussion has been given elsewhere.[15] The lattice parameters of $LaSb_2$, $CeSb_2$, $NdSb_2$, and $SmSb_2$ are shown in Table V and were calculated by a least-squares refinement of their powder diffraction data obtained with Cu Kα radiation, λ 1.542 A.

The volumes permit the placement of 8 formula weights in the unit cell. The systematic extinctions showed that the most probable space group was Cmca or C2ca and the structure refinement indicates that the former is correct.

Single-crystal diffraction patterns of $LaSb_2$ always showed an intensity distribution along festoons of spots when h was odd and different preparative procedures never produced ordered crystals. The crystals of $SmSb_2$ were ordered and therefore they were used to solve the structure.

A single crystal of $SmSb_2$ with dimensions 0.05 × 0.06 × 0.02 mm was mounted along the y axis. In order to obtain the maximum number of reflections and smaller absorption errors ($\mu_{Cu\,K\alpha}$ = 2470 cm^{-1}, $\mu_{Mo\,K\alpha}$ = 232.0 cm^{-1}), Mo Kα radiation was used. Intensity data for $h0l$, $h1l$, $h2l$, $h3l$, and $h4l$ were obtained from multiple Weissenberg films. The peak intensities were read by comparison with a standard intensity scale. The reflections were corrected for Lorentz and polarization effects and also for absorption. The procedure for ultimately bringing all reflections to the same scale was the same as previously described for the $ErSe_2$ data.

The values of the cell constants indicated that the structures of $LaSb_2$ type phases were closely related to both $RETe_2$ (Fe_2As) and $YbSb_2$ ($ZrSi_2$) type structures. The following relationships were evident: $a_{LaSb_2} \cong b_{LaSb_2} \cong \sqrt{2}a_{LaTe_2}$, $c_{LaSb_2} \cong 2c_{LaTe_2}$, $a_{LaSb_2} \cong \sqrt{2}a_{YbSb_2}$, $b_{LaSb_2} \cong \sqrt{2}c_{YbSb_2}$, and $c_{LaSb_2} \cong b_{YbSb_2}$.

These relationships suggest a comparison of the $h0l$ reciprocal lattice of $SmSb_2$ with the hhl lattice of $LaTe_2$. Both the observed extinctions and intensities indicated that $SmSb_2$ in the (010) projection has the same structural arrangement as that found in $LaTe_2$ projected along [110]. The 0, y, and z parameters obtained from the $0kl$ Patterson map were similar to those found in the $YbSb_2$ structure, and therefore the same applicable atomic positions as in $LaTe_2$ and $YbSb_2$ were used as the initial parameters for the calculations of $h0l$ and $0kl$ structure factors, respectively. The z parameters from the $LaTe_2$ structure are equivalent to the y parameters in $YbSb_2$ after they are shifted by $^1/_4$ along the long axis of the unit cell. Regularity in the stacking requires that all of the z parameters of the $LaTe_2$ structure be increased by $^1/_4$; these changes affect only the signs of $F(h0l)$. The trial structure gave a satisfactory R factor of 0.14 for $h0l$ while for $0kl$ the R factor was 0.20. At this stage the structure was refined by least squares[17] using 197 observed independent hkl reflections with unit weights. The scattering factors for Sm and Sb obtained from the "International Tables for X-Ray Crystallography,"[16] modified for the real part of the dispersion correction, were used in the calculations. The final parameters and anisotropic temperature factors are shown in Table VI and F_o and F_c are listed in Table VII. The discrepancy coefficient is 0.080 for observed reflections greater than zero, and the calculated standard deviation of an observation of unit weight is 1.15.

(18) J. S. Anderson, *J. Chem. Soc.*, 43, 104 (1946).

TABLE V

CRYSTAL DATA OF $LaSb_2$, $CeSb_2$, $NdSb_2$, AND $SmSb_2$

	a, A	*b*, A	*c*, A	Vol, A³	D_m, g/cc	D_x, g/cc
$LaSb_2$	6.314 ± 0.005	6.175 ± 0.005	18.56 ± 0.01	725.1	6.68	7.00
$CeSb_2$	6.295 ± 0.006	6.124 ± 0.006	18.21 ± 0.02	702.2	6.69	7.25
$NdSb_2$	6.207 ± 0.004	6.098 ± 0.004	18.08 ± 0.01	684.3	6.82	7.53
$SmSb_2$	6.171 ± 0.006	6.051 ± 0.006	17.89 ± 0.02	668.0	7.56	7.83

TABLE VI

FINAL ATOMIC PARAMETERS FOR $SmSb_2$[a]

	x	*y*	*z*	B_{11}[b]	B_{22}	B_{33}	B_{13}	B_{23}
Sm	0	0.3653	0.3902	0.0037	0.0080	0.0074	...	0.0007
		(0.0013)	(0.0002)	(0.0006)	(0.0017)	(0.0001)		(0.0005)
Sb(1)	0	0.8686	0.4360	0.0044	0.0031	0.0008	...	−0.0002
		(0.0017)	(0.0002)	(0.0008)	(0.0020)	(0.0001)		0.0006)
Sb(2)	0.25	0.1222	0.25	0.0053	−0.0024	0.0008	0.0001	...
		(0.0028)		(0.0007)	(0.0015)	(0.0001)	(0.0002)	

[a] Numbers in parentheses are the standard deviations. B_{12} is zero for all atoms. [b] The anisotropic temperature factor expression is $\exp[-(B_{11}h^2 + B_{22}k^2 + B_{33}l^2 + 2B_{12}hk + 2B_{13}hl + 2B_{23}kl)]$.

TABLE VII

OBSERVED AND CALCULATED STRUCTURE FACTORS FOR $SmSb_2$[a]

l	F_o	F_c
h = 0, k = 0		
2	0	-29
4	0	-67
6	796	-800
8	304	270
10	176	-160
12	117	137
14	301	-305
16	386	382
18	174	145
20	194	177
22	375	-377
h = 0	k = 2	
0	0	-64
1	0	47
2	0	-41
3	815	981
4	71	55
5	142	-150
6	66	36
7	0	34
8	0	7
9	334	-404
10	0	-33
11	246	295
12	0	9
13	265	-283
14	0	11
15	0	-46
16	0	1
17	222	-237
18	0	-34
19	344	394
h = 0	k = 4	
0	750	-819
1	0	-80
2	0	48
3	0	-82
4	0	2
5	0	-39
6	633	570
7	0	74
8	219	-207
9	0	18
10	168	161
11	0	-4
12	146	-130
13	0	-27
14	245	245
15	0	44
16	304	-332
17	0	16
18	54	-94
19	0	-16
20	194	-154
h = 1	k = 1	
1	0	1
2	0	134
3	220	-222
4	135	-129
5	152	-160
6	376	-395
7	225	222
8	185	-168
9	483	387
10	259	283
11	76	96
12	384	368
13	305	-238
14	71	47
15	206	-223
16	214	-196
17	0	3
18	113	-123
19	96	86
h = 1	k = 3	
1	0	-12
2	0	64
3	212	208
4	112	-103
5	168	164
6	261	-261
7	211	-212
8	102	-99
9	378	-396
10	209	202
11	122	-108
12	273	250
13	295	251
14	0	28
15	288	248
16	135	-129
h = 2	k = 0	
0	453	421
2	597	638
4	650	-694
6	108	-127
8	276	-290
10	339	342
12	339	-312
14	123	105
16	0	11
18	430	449
20	150	-102
22	152	-123
24	338	-301
h = 2	k = 2	
0	129	-80
1	570	654
2	0	-15
3	320	288
4	0	29
5	444	428
6	0	53
7	511	-500
8	0	-11
9	117	113
10	0	-14
11	180	-167
12	0	-6
13	163	136
14	0	24
15	379	-406
16	0	-10
17	0	94
18	0	-21
19	0	91
20	0	-17
21	360	380
h = 2	k = 4	
0	306	-249
1	0	-38
2	499	-467
3	0	-113
4	544	502
5	0	-1
6	0	58
7	0	36
8	249	254
9	0	48
10	268	-268
11	0	-33
12	249	263
13	0	
14	0	-118
h = 3	k = 1	
1	0	5
2	127	112
3	199	-179
4	118	-103
5	147	-135
6	327	-330
7	189	188
8	136	-146
9	297	334
10	243	248
11	81	85
12	348	325
13	198	-214
14	0	43
15	154	-199
16	159	-180
17	0	2
18	99	-111
h = 3	k = 3	
1	0	-13
2	0	57
3	133	180
4	89	-89
5	150	145
6	241	-228
7	178	-186
8	83	-89
9	306	-350
10	189	182
11	113	-98
12	246	224
13	226	228
14	0	26
15	206	224
16	128	-120
h = 4	k = 0	
0	811	822
2	0	-12
4	0	-59
6	601	-561
8	210	200
10	149	-113
12	111	102
14	249	-246
16	324	309
18	180	125
20	0	148
22	335	-321
h = 4	k = 2	
0	93	-46
1	0	42
2	0	-29
3	655	700
4	0	40
5	124	-108
6	0	27
7	0	15
8	0	4
9	325	-308
10	0	-26
11	240	235
12	0	7
13	218	-222
14	0	9
15	0	-43
16	0	1
17	194	-197
18	0	-28
19	322	330
h = 4	k = 4	
0	601	-640
1	0	-63
2	0	33
3	0	-66
4	0	9
5	0	-30
6	411	452
7	0	60
8	183	-167
9	0	15
10	168	124
11	0	-4
12	159	-103
13	0	-23
14	204	204
15	0	37
16	243	-277
h = 5	k = 1	
1	0	7
2	79	88
3	124	-138
4	81	-75
5	99	-106
6	249	-259
7	152	145
8	114	-116
9	262	259
10	198	197
11	77	67
12	253	268
13	153	-175
14	0	32
15	134	-168
16	137	-150
h = 5	k = 3	
1	0	-14
2	0	48
3	118	144
4	83	-68
5	124	118
6	182	-185
7	173	-148
8	97	-71
9	288	-289
10	145	147
11	102	-79
12	195	188
13	183	190
14	0	19
15	189	191
h = 6	k = 0	
0	267	250
2	387	351
4	416	-402
6	0	-86
8	167	-166
10	208	220
12	207	-204
14	0	60
16	0	11
18	316	321
h = 6	k = 2	
0	0	-48
1	420	388
2	0	-9
3	204	186
4	0	19
5	263	253
6	0	33
7	325	-317
8	0	-7
9	0	67
10	0	-10
11	0	-98
12	0	-3
13	0	91
14	0	17
15	287	-283
h = 6	k = 4	
0	172	-175
1	0	-26
2	267	-303
3	0	-76
4	322	334
5	0	-1
6	0	47
7	0	26
8	144	163
9	0	33
10	168	-186
11	0	-24
12	185	183
h = 7	k = 1	
1	0	8
2	77	70
3	111	-103
4	60	-55
5	93	-84
6	206	-195
7	89	110
8	97	-92
9	191	205
10	161	154
11	0	54
12	202	207
13	131	-141
h = 7	k = 3	
1	0	-13
2	0	39
3	127	110
4	0	-51
5	107	95
6	132	-142
7	123	-115
8	0	-58
9	220	-225
10	133	118
11	0	-65
12	164	146
13	166	154
14	0	17
15	114	151
h = 8	k = 0	
0	464	445
2	0	1
4	0	-47
6	293	-310
h = 8	k = 2	
0	0	-27
1	0	35
2	0	-16
3	399	392

[a] Unobserved values are listed as zero and were not used in the refinement and in the calculation of *R*.

Discussion of the Structure

The $LaSb_2$ type structure is essentially derived from the $RETe_2$ (Fe_2As) and $YbSb_2$ ($ZrSi_2$) structures. The projections on (010) and (100) are shown in Figure 1 from which it can be seen that the former projection is the same as the$RETe_2$ structure projected on (110) and the latter is analogous to the (101) projection of $YbSb_2$. The structure is formed by ten layers of atoms stacked in the order Sb(1), RE, Sb(2), RE, Sb(1), Sb(1), RE, Sb(2), RE, Sb(1). The stacking sequence and the population of atoms in each layer are analogous to those in $YbSb_2$.

The bond distances for $SmSb_2$ are given in Table VIII. Each Sm atom has four nearest Sb(1) atoms forming a slightly distorted square 0.82 A below it and four Sb(2) basal atoms which form a rectangular layer of size $\frac{1}{2}a_0 \times \frac{1}{2}b_0$ 2.50 A above it and rotated 45° with respect to the Sb(1) square, Figure 2(a) [in ref 5 the atom in the basal plane is labeled Te(1)]. The coordination polyhedron around Sm has also one Sb(1) atom at a distance of 3.479 A and another Sm atom at a distance of 4.198 A, which lie below the square formed by the Sb(1) layer. Owing to the screening effect of this Sb(1) layer, the Sm–Sm distance is too large to assume bonding. Each Sb(1) atom is surrounded by four Sm atoms which form a slightly distorted square 0.82 A above it, and at a vertical distance of 3.33 A are four Sb(2) atoms located above the square of Sm atoms, Figure 2(b). The Sb(1)–Sb(2) distances are about 3.97 A so that there is no contact between them. The Sb(1) atom is also coordinated by another Sb(1) atom and one Sm atom below it at 2.720 and 3.479 A, respectively. The 2.720-A separation of Sb(1)–Sb(1) is considerably shorter than the 2.87-A distance found in elemental Sb. One Sb(2) atom is located in the center of four nearest Sb(2) atoms within the same layer forming a rectangle of size $a_0 \times b_0$, Figure 2(c). The Sb(2) atoms are also coordinated by two Sm atoms at a distance of 3.300 A and two Sm atoms at 3.319 A.

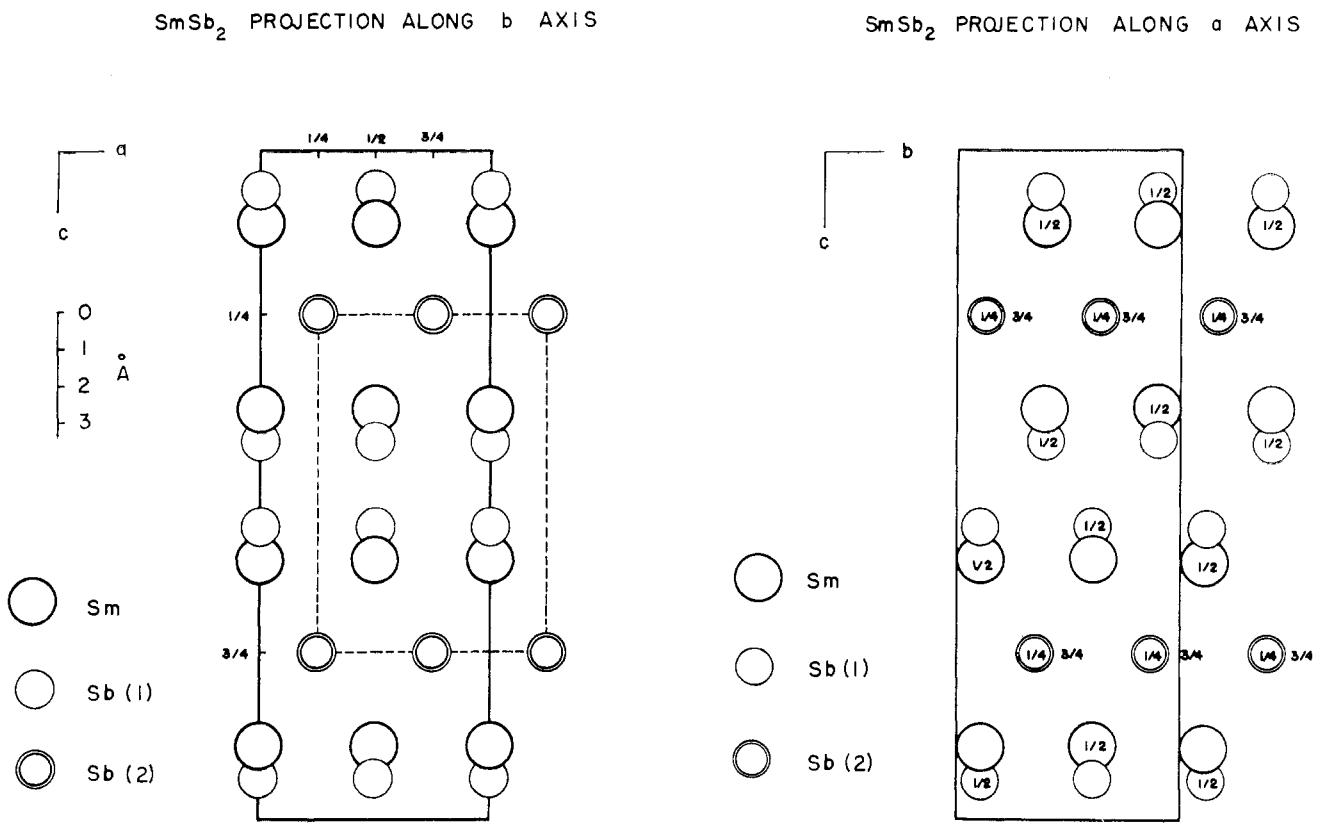

Figure 1.—The crystal structure of $SmSb_2$ projected on the (010) and (100) planes.

TABLE VIII
INTERATOMIC DISTANCES AND THEIR STANDARD DEVIATIONS FOR $SmSb_2$, A

Sm–Sm	4.198 ± 0.016	Sb(1)–Sm	3.479 ± 0.018
Sm–2Sb(1)	3.193 ± 0.018	Sb(1)–Sb(1)	2.720 ± 0.021
Sm–Sb(1)	3.134 ± 0.018	Sb(1)–2Sb(2)	3.973 ± 0.021
Sm–Sb(1)	3.136 ± 0.018	Sb(1)–2Sb(2)	3.959 ± 0.021
Sm–Sb(1)	3.479 ± 0.018	Sb(2)–2Sm	3.319 ± 0.018
Sm–2Sb(2)	3.319 ± 0.018	Sb(2)–2Sm	3.300 ± 0.018
Sm–2Sb(2)	3.300 ± 0.018	Sb(2)–2Sb(1)	3.973 ± 0.021
Sb(1)–2Sm	3.193 ± 0.018	Sb(2)–2Sb(1)	3.959 ± 0.021
Sb(1)–Sm	3.136 ± 0.018	Sb(2)–2Sb(2)	3.086 ± 0.021
Sb(1)–Sm	3.134 ± 0.018	Sb(2)–2Sb(2)	3.026 ± 0.021

Discussion

A listing of the three series which we investigated is shown in Table IX; the structure types are given, and the absent phases are enclosed by dashed lines.

TABLE IX

$LaSe_2$	$LaSe_2$ type	$LaTe_2$	Fe_2As type	$LaSb_2$	$LaSb_2$ type
$CeSe_2$		$CeTe_2$		$CeSb_2$	
$NdSe_2$		$NdTe_2$		$NdSb_2$	
$SmSe_2$		$SmTe_2$		$SmSb_2$	
$GdSe_2$		$GdTe_2$		$GdSb_2$	
$DySe_2$	$ErSe_2$ type	$DyTe_2$		$DySb_2$	
$HoSe_2$		$HoTe_2$		$HoSb_2$	
$ErSe_2$		$ErTe_2$		$ErSb_2$	
$YbSe_2$		$YbTe_2$	Fe_2As type	$YbSb_2$	($ZrSi_2$)

An examination of the occurrence of absent phases shows that within the same series the stability of the structure is governed by the behavior of the rare earth elements. If in the formation of the structure there is a discontinuity at one rare earth element, the structure will not be formed again for the remaining trivalent rare earth elements and a new structure may be formed if the later rare earth elements provide suitable sizes or valences. If the discontinuity occurs at an element which has the same valence as its adjacent neighbors, the size factors will be the main reason for the absence of these phases.

Single phases of $HoTe_2$ and $ErTe_2$ could not be obtained in this investigation and only mixtures of the two phases of compositions 1:1 and 1:3 were obtained. In order to explain the absence of $HoTe_2$ and $ErTe_2$, the structure of $HoTe_3$ and $ErTe_3$ must be discussed and the relationship between the $RETe_2$ and $RETe_3$ structures needs to be understood.

The structure of $RETe_3$ consists of a stacking of slightly distorted $RETe_2$ units which have an additional tellurium layer between adjacent unit cells stacked along the z direction, with alternate cells shifted by $^1/_2a$.[19] The coordination around the RE atoms in $RETe_3$ is identical with the one in $RETe_2$ except for small differences in bond lengths. These small differences are the main reason why $ErTe_3$ and $HoTe_3$ are formed rather than the ditellurides. The unit cell constants for $LaTe_3$,[20,21] $NdTe_3$,[11,19,21] and $ErTe_3$[21,22] are

(19) B. K. Norling and H. Steinfink, *Inorg. Chem.*, **5**, 1488 (1966).
(20) T. H. Ramsey, H. Steinfink, and E. J. Weiss, *ibid.*, **4**, 1154 (1965).
(21) M. P. Pardo, O. Gorochov, J. Flahaut, and L. Domange, *Compt. Rend.*, **260**, 1666 (1965).
(22) D. J. Haase, H. Steinfink, and E. J. Weiss, *Inorg. Chem.*, **4**, 541 (1965).

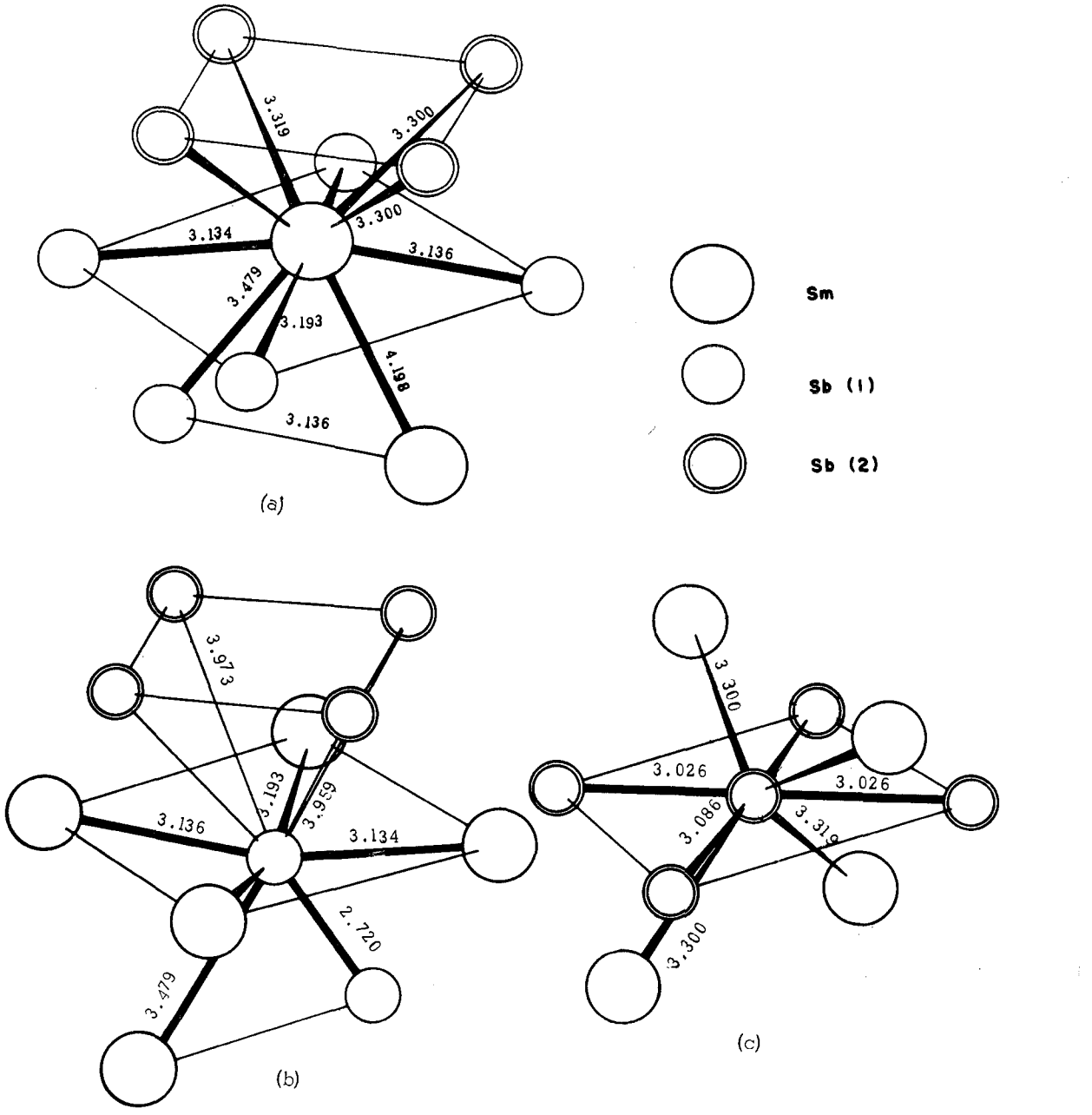

Figure 2.—(a) The coordination polyhedron around Sm in $SmSb_2$; (b) the coordination polyhedron around Sb(1) in $SmSb_2$; (c) the coordination polyhedron around Sb(2) in $SmSb_2$.

$LaTe_3$	a_0 = 4.41 A	c_0 = 26.14 A
$NdTe_3$	a_0 = 4.35 A	c_0 = 25.80 A
$ErTe_3$	a_0 = 4.31 A	c_0 = 25.45 A

The a_0 parameters of $RETe_3$ are essentially the same as for $RETe_2$ while the c_0 parameters are approximately tripled in the $RETe_3$ structure. A comparison of the values of a_0 for $LaTe_3$ with those for $ErTe_3$ shows that they shrink 0.1 A whereas the shrinkage from $LaTe_2$ to $DyTe_2$ is 0.24 A. If $HoTe_2$ and $ErTe_2$ existed, the a_0 axis for $HoTe_2$ should be 4.28 A, and for $ErTe_2$ 4.27 A obtained from the extrapolation of the $RETe_2$ lattice parameter curves to Ho and Er. Thus the shrinkage of a_0 will be 0.26 A from $LaTe_2$ to the hypothetical $ErTe_2$.

The length of the a_0 axis is mainly governed by the Te–Te contacts in the basal plane. The Te atoms in the $RETe_2$ structure are coordinated by two layers of RE atoms, one on each side. As the rare earth element changes from La to Er, the smaller size of the Er atoms compresses these Te atoms closer together. In the $RETe_3$ structure, the compressive force on the Te layer is greatly reduced because each Te layer is only coordinated with one layer of RE atoms. Therefore, in $HoTe_3$ and $ErTe_3$ a reasonable bond length for Te–Te can be retained while this distance becomes too short in $HoTe_2$ (3.015 A) and $ErTe_2$ (3.005 A) and thus makes the structure unstable. The Te–Te distance could be maintained at a proper value if the angle Te–RE–Te increased as the rare earth atom size decreased. However, this would lead to a decrease in the distance between the rare earth atoms on each side of the tellurium layer and to an increased electrostatic repulsive force,

and the structure again becomes unstable. The compression of Te atoms in the structure is relieved by the introduction of an additional Te layer in the $HoTe_2$ and $ErTe_2$ phases, and the stoichiometry changes to $HoTe_3$ and $ErTe_3$. The Te–Te distance in $ErTe_3$ is increased to 3.045 A which is equivalent to the separation observed in $TbTe_2$.

It can be predicted from the size effect that $TmTe_2$ and $LuTe_2$ cannot be formed and that $TmTe_3$ is possible[21] since it will have a Te–Te separation of 3.030 A which is the limiting distance in $DyTe_2$. $LuTe_3$ will be absent since the Te–Te distances will be 3.015 A which is in a range where no structure is formed.

The rare earth elements and antimony form primarily rare earth rich phases. In the La–Sb and Yb–Sb phase diagrams, $LaSb_2$ and $YbSb_2$ were found as the only Sb-rich phases, and it can be inferred that if the size factor is no longer favorable to form the $LaSb_2$ or $YbSb_2$ structure types for other $RESb_2$ phases, then no other Sb richer phases will be formed.

A study of the ternary phases on the sections $LaSb_2$–$LaTe_2$ and "$LaSn_2$"–$LaSb_2$ showed that the $LaSb_2$ structure was very unstable in ternary alloys.[23] The formation of this structure requires very critical conditions of valence, electrochemical nature, and atomic size. Since Gd, Dy, Ho, and Er have the same trivalent oxidation state and similar electronegativities as the elements forming the $LaSb_2$ type structure, the size relationship should be considered as the only important factor which is responsible for the absence of some rare earth diantimonides.

The shortest Sb–Sb separations are 2.803 A in $LaSb_2$, 2.760 A in $CeSb_2$, 2.742 A in $NdSb_2$, and 2.720 A in $SmSb_2$. Assuming that $GdSb_2$, $DySb_2$, $HoSb_2$, and $ErSb_2$ can crystallize in the $LaSb_2$ structure, their lattice parameters can be obtained by extrapolating the lattice constant for the $RESb_2$ phases, and probable Sb–Sb distances can be computed. The Sb–Sb separation should thus be 2.704 A in $GdSb_2$, 2.690 A in $DySb_2$, 2.681 A in $HoSb_2$, and 2.671 A in $ErSb_2$. The shortest Sb–Sb separation that can be found from other antimonides is 2.81 A which is similar to that in $LaSb_2$. The separation of Sb–Sb in $GdSb_2$ is 0.016 A shorter than that found in $SmSb_2$. A 0.015-A contraction in the atomic separation in the Te–Te bond leads to the absence of $HoTe_2$ and similarly such a decrease in Sb–Sb prevents the $RESb_2$ crystallization from Gd onward.

Nature of Bonding

With a knowledge of interatomic distances and coordination configurations, it is possible to deduce the nature of the bonds between particular atoms in the structures. The rare earth atom is coordinated by nine Te or Se atoms in $RETe_2$ and $RESe_2$ and by ten Sb atoms in the $RESb_2$ structure. Since there is no RE–RE contact, no pure metallic bond is formed. The RE–B bond is essentially a mixed bond of metallic and covalent character with a slight ionic contribution. The percentage contributions of each bond type can be calculated using an empirical formula adopted by Miller, *et al.*[12] From a knowledge of the radii, an estimate of the bond character can be calculated by the relationship

$$\%\ \text{covalent (metallic)} = \frac{[r(\text{iron}) - r(\text{app})] \times 100}{r(\text{ion}) - r((\text{covalent})\,(\text{metallic}))}$$

where r(ion), r((covalent) (metallic)), and r(app) are the ionic, covalent (metallic), and apparent radii of the B atoms and rare earths, respectively.

The method for obtaining a value of the apparent radius for a particular element is illustrated for $SmSb_2$. The average value of the shortest Sm–Sb distance, for which the atoms are considered to be in contact, is 3.24 A. Similarly Sb–Sb contact is considered to exist for the distance 2.94 A; r(app) for Sb is thus 1.47 A and for Sm it is 1.77 A. The per cent covalent character for the Sm–Sb bond is thus 96% using 1.04 A for the ionic radius of Sm^{3+} and 1.804 A for its metallic radius. The assumption is made that the atoms have the same positions in a given structure type so that the values of the apparent radii for compounds in which the rare earth atom changes are governed by the changes of the cell constants. The calculated metallic bond character values for $LaSe_2$, $LaTe_2$, and $LaSb_2$ are 69, 76, and 93%, respectively, and the increase in these values with the atomic number of the rare earth atom merely reflects the changes in the lattice constants.

Quantitative discussions of the electrical transport properties of metals and semiconductors usually involve a band model for the structure, but it is also reasonable to interpret these properties as due to the mixed ionic–metallic–covalent bond as previously pointed out by Mooser and Pearson.[24] From an examination of the structural arrangements and the bond character in these compounds, $RESe_2$, and $RETe_2$ should be classified as semiconductors and $RESb_2$ should just enter into the metallic category. The semiconducting properties of $LaSe_2$,[25] $CeSe_2$,[12] $LaTe_2$,[26] and $GdTe_2$[12] have been studied, and the room-temperature resistivity of 79 μohm-cm for $YbSb_2$ measured in this laboratory indicates the nearly metallic character of this phase. Only the $LaSb_2$ type compounds require further work to show the consistency between the electronic properties and the bond character.

(23) R. Wang, H. Steinfink, and A. Raman, *Inorg. Chem.*, **6**, 1298 (1967).

(24) E. Mooser and W. B. Pearson, *Phys. Rev.*, **101**, 1608 (1965).

(25) V. A. Obolonchick and G. V. Lashkarew, "Production, Properties and Prospects of Utilization of Selenides of the Rare Earth Metals in Problems of the Theory and Use of the Rare Earth Metals," Y. M. Savitsky and V. F. Tereknova, Ed., Science Publishing House, Moscow, 1964.

(26) T. H. Ramsey, H. Steinfink, and E. J. Weiss, *J. Appl. Phys.*, **36**, 548 (1965).